JOURNAL OF GEOPHYSICAL RESEARCH, VOL. 104, NO. D18, PAGES 22,195–22,203, SEPTEMBER 27, 1999

On the relationship among cloud turbulence, droplet formation and drizzle as viewed by Doppler radar, microwave radiometer and lidar

Graham Feingold and A. Shelby Frisch

Cooperative Institute for Research in the Atmosphere/NOAA, Environmental Technology Laboratory
Boulder, Colorado

Bjorn Stevens

Department of Atmospheric Sciences, University of California, Los Angeles

William R. Cotton

Department of Atmospheric Science, Colorado State University, Fort Collins

Abstract. Cloud radar, microwave radiometer, and lidar remote sensing data acquired during the Atlantic Stratocumulus Transition Experiment (ASTEX) are analyzed to address the relationship between (1) drop number concentration and cloud turbulence as represented by vertical velocity and vertical velocity variance and (2) drizzle formation and cloud turbulence. Six cases, each of about 12 hours duration, are examined; three of these cases are characteristic of nondrizzling boundary layers and three of drizzling boundary layers. In all cases, microphysical retrievals are only performed when drizzle is negligible (radar reflectivity <-17 dBZ). It is shown that for the cases examined, there is, in general, no correlation between drop concentration and cloud base updraft strength, although for two of the nondrizzling cases exhibiting more classical stratocumulus features, these two parameters are correlated. On drizzling days, drop concentration and cloud-base vertical velocity were either not correlated or negatively correlated. There is a significant positive correlation between drop concentration and mean in-cloud vertical velocity variance for both nondrizzling boundary layers (correlation coefficient $r = 0.45$) and boundary layers that have experienced drizzle ($r = 0.38$). In general, there is a high correlation ($r > 0.5$) between radar reflectivity and in-cloud vertical velocity variance, although one of the boundary layers that experienced drizzle exhibited a negative correlation between these parameters. However, in the subcloud region, all boundary layers that experienced drizzle exhibit a negative correlation between radar reflectivity and vertical velocity variance.

1. Introduction

Over the past decades the relationship between cloud droplet number (N) concentration and cloud condensation nucleus (CCN) concentration has been the focus of extensive studies. Anthropogenic sources of aerosol particles, some fraction of which are CCN, are expected to generate clouds that are more reflective and are less apt to precipitate. *Twomey* [1959] proposed a power law activation spectrum

$$N = CS^k, \tag{1}$$

where N is the number of drops activated at supersaturation S, and C and k are measured parameters related to the number of CCN and the slope of the size distribution. (More specifically, C is the number of drops activated at $S = 1\%$.) Although (1) is only approximate, it serves to illustrate the relative importance of C and the updraft velocity w in determining N. *Twomey* [1977] showed that for $k \approx 0.5$, there is a strong correlation between N and C, with a much weaker correlation between N and w. However, the relationship between N and w remains unclear since it depends on k; for spectra with steep slopes (large k), w plays an increasingly important role in determining N [e.g., *Leaitch et al.*, 1996], whereas for spectra with shallow slopes (small k), N is determined primarily by C. In reality, the CCN activation spectrum is far more complex than that described by (1), and the value of k has been shown to increase with decreasing S (or increasing particle size) [*Hudson*, 1984]. Over the range of particle sizes (0.1 μm, 1 μm), k tends to be larger than it is for particles <0.1 μm. One of the goals of this note is to investigate the relationship between N and w, or some measure of cloud turbulence, without the restrictive assumptions of (1).

Another interesting link between cloud and boundary layer dynamics is the one between cloud turbulence and drizzle formation [*Bowen*, 1950; *Mason*, 1952; *Austin et al.*, 1995; *Feingold et al.*, 1996]. A variety of models ranging from simple conceptual models to large eddy simulations coupled with bin microphysical models, have shown that clouds that exhibit higher turbulence kinetic energy can sustain drops within cloud for longer periods of time and promote drizzle formation through collision-coalescence. To the best of our knowledge this hypothesis has not been placed on firm observational ground.

Paper number 1999JD900482.
0148-0227/99/1999JD900482$09.00

Finally, a related issue is the impact that drizzle has on boundary layer dynamics [e.g., *Paluch and Lenschow*, 1991; *Feingold et al*., 1996; *Stevens et al*., 1998]. These studies have indicated that drizzle tends to stabilize the boundary layer and suppress turbulence. A transition from a stratus to a "cumulus-like" cloud regime is indicated. An exception may exist where small amounts of drizzle cool the region just below cloud base and destabilize the boundary layer [*Feingold et al*., 1996; *Stevens et al*., 1998].

The goal of this note is to present observational data pertaining to these three issues, namely (1) the relationship between cloud turbulence and drop number concentration, (2) the causal relationship between cloud turbulence and drizzle formation, and (3) the impact of drizzle on boundary layer turbulence. The key instruments are the NOAA K_α-band Doppler radar in combination with a NOAA microwave radiometer. As described below, together they provide an effective tool for simultaneously measuring both microphysical and dynamical parameters and shedding light on the close coupling of cloud microphysics and boundary layer dynamics.

2. Instrumentation

The primary instruments used in this study are the NOAA Environmental Technology Laboratory K_α-band (8.6 mm) Doppler radar [*Kropfli et al*., 1995] and the microwave radiometer [*Hogg et al*., 1983]. The data set is augmented by the NOAA 10.59 μm Doppler lidar [*Pearson*, 1993]. The instruments were deployed on the island of Porto Santo in the eastern Atlantic Ocean for the duration of the Atlantic Stratocumulus Transition Experiment (ASTEX) in 1992. The instruments have been described in detail elsewhere; most pertinent to this study is the fact that the K_α-band radar has high sensitivity and is therefore ideally suited to stratus cloud studies. The primary product of the microwave radiometer used here is the derived liquid water path (LWP). The lidar is used as an indicator of cloud base because the strong size-weighting (drop size to the power of 6) of the radar signal tends to underestimate cloud-base height whenever precipitation-sized drops are present.

The typical radar scanning strategy during ASTEX consisted of a 23–25 min record of vertically pointing data followed by 5–7 min of conical scanning. Only vertically pointing data are used here. Doppler vertical velocity w and radar reflectivity Z were measured at 3 s temporal resolution, whereas the vertically pointing microwave radiometer recorded data at 1 min resolution. The lidar, which is only used here as an indicator of cloud base, recorded data at 1 s intervals. Cloud top is deduced from the radar using a detection threshold of -35 dBZ.

2.1. The w and σ_w^2 Measurements

The w field has been analyzed with the following caveats: drizzle events (defined as data where $Z > -17$ dBZ) have been precluded from the analysis because the occurrence of drizzle, and associated terminal velocities of large drops, contaminates the w measurement. In addition, w data in regions where the signal-to-noise ratio is low have been excluded. Although the cloud radar measured the second moment (variance) of the velocity spectrum, these data were deemed unreliable for the goals of this study because at low signal-to-noise ratios the noise contaminates the measurement and generates spuriously high variance [*Gibson*, 1988]. Instead, the vertical velocity variance σ_w^2 has been calculated from a time series of instantaneous w measurements as in the work of *Frisch et al*. [1995a]. The duration of this time series is of the order of 25 min to a few hours. In calculating σ_w^2, w data have been corrected for the mean velocity during the course of the observation period,

$$\sigma_w^2 = \frac{1}{N_s - 1} \sum_j (w_j - \bar{w})^2, \tag{2}$$

where $\bar{w}$ is the mean updraft velocity, N_s is the number of samples, and j is the index pertaining to the time series. Although, ideally, $\bar{w}$ should average to zero after sufficient sampling, this is not always the case [e.g., *Lenschow et al*., 1994].

2.2. Description of the Microphysical Retrieval

Central to this study is a method for retrieving cloud liquid water content and droplet microphysical parameters, as discussed by *Frisch et al*. [1995b]. Used in tandem, the vertically pointing K_α-band Doppler radar and microwave radiometer provide a measure of N, characteristic size, and liquid water content (LWC) profiles in nonprecipitating clouds. The cloud droplet size distribution is assumed to conform to a lognormal distribution with three parameters: N the droplet concentration, r_g the geometric mean radius, and σ the geometric standard deviation.

Radar data are averaged over 1 min to match the radiometer resolution, and profiles of LWC are derived from range-gated radar reflectivity Z_i measurements (at 37.5 m vertical resolution) together with the radiometer-derived LWP. N is also retrieved assuming that it is invariant with height (a reasonable assumption for nonprecipitating marine stratocumulus clouds with weak shear [*Nicholls*, 1984]), and the breadth of the size distribution σ is a fixed constant. In this work, a σ of 1.2 has been assumed, which is appropriate for nonprecipitating clouds; *Atlas* [1954] used a breadth parameter X with a value equivalent to $\sigma = 1.2$, and *Paluch et al*. [1996] derived a value of X equivalent to $\sigma = 1.16$ for nonprecipitating small cumuli. These values are different from the value of 1.42 assumed by *Frisch et al*. [1995b].

Comparisons of this remote sensing technique with in situ data [*Frisch et al*., 1999] indicate excellent retrieval of cloud water content. However, the retrieved value of N is very sensitive to the assumed value of σ, so N is only qualitatively correct. For example, *Frisch et al*. [1995b] show that

$$N = f(\mathrm{LWP}, Z_i) e^{9\ln^2\sigma}, \tag{3}$$

where $f(\mathrm{LWP}, Z_i)$ is a function of LWP and the radar reflectivity profile. Let us assume that $f(\mathrm{LWP}, Z_i) = 74$ cm^{-3}, which yields $N = 100$ cm^{-3} at $\sigma = 1.2$. Now, if σ were only 1.1 rather than the assumed value of 1.2, then $N = 80$ cm^{-3}, i.e., an error of 20% in N. If, on the other hand, $\sigma = 1.3$ rather than 1.2, then $N = 137$ cm^{-3}, i.e., an error of 37%. At $\sigma = 1.4$, the error increases to about 100%. However, we note that the error in N for a given relative error in σ increases with increasing σ,

$$\frac{dN}{N} \propto \ln \sigma \, \frac{d\sigma}{\sigma}, \tag{4}$$

so the fact that we are looking at nonprecipitating clouds with rather narrow spectra ($\sigma \approx 1.2$) tends to mitigate the errors. Regardless, we caution against making inappropriate quantitative inferences.

In spite of the difficulty in quantifying N, the fact that large samples can be analyzed with this method is of great advantage. If sufficient averaging of these data is performed and robust relationships between various measured parameters are obtained, then these relationships are expected to be meaningful. We attempt here to seek such relationships and to interpret their significance. In addition, we wish to examine whether there are differences between nondrizzling boundary layers and boundary layers that have experienced drizzle.

3. Results

In this study, six events have been analyzed; three of these have been defined as nondrizzling events June 13, 14, and 18, and three as drizzling events, June 12, 17 (before noon) and 17 (after noon). The duration of these events is indicated in Table 1. These events were chosen from the full data set by selecting periods that filled a number of criteria, including significant cloud cover, significant duration of drizzle, and high signal-to-noise ratio in the radar data. Analyses for the nondrizzling and drizzling cases are compared.

3.1. Relationship Between N and Cloud Base w

Figure 1 shows N as a function of the positive (upward) Doppler velocity values at cloud-base w_{cb} for all six days. Note that w_{cb} represents a 1 min average of the individual w measurements (positive and negative) and as such is representative of a length scale of about 300 m for typical boundary layer horizontal winds of 5 m s^{-1}. This spatial scale may be too large to capture all activation events, as discussed in section 4.1. The correlation coefficient r is shown to be 0.07, indicating no significant relationship between N and w_{cb}. Similar results were arrived at by plotting N versus maximum updraft velocity (data not shown). Superimposed on Figure 1 are theoretical calculations of N versus w_{cb} derived from an adiabatic parcel model representing droplet activation for two different CCN input spectra: (1) a narrow spectrum with a concentration of 1000 cm^{-3} and median radius of 0.05 μm and (2) a broad spectrum with a concentration of 50 cm^{-3} and median radius of 0.1 μm. As expected, N is more strongly dependent on w_{cb} for the steeper, narrow spectrum. Separating the data by case (Figure 2) shows that in general, the nondrizzling days show a small positive correlation between N and w_{cb}, whereas the drizzling days show very small negative correlation between these two parameters. Only June 18 indicates fairly good positive correlation between w_{cb} and N ($r = 0.47$). On any given day there is significant variability in N. Some of this probably derives from variability in the CCN concentration and size distribution, while some is related to inaccuracies in the retrieval (including sensitivity to σ and instrument calibration). The existence of data points at high N and low w_{cb} may occur when there is no link between N and w_{cb}; that is, the drops were previously activated and are being recirculated by the cloud. Data points at low N and high w_{cb} may be explained by local depletion in CCN resulting from prior activation scavenging events.

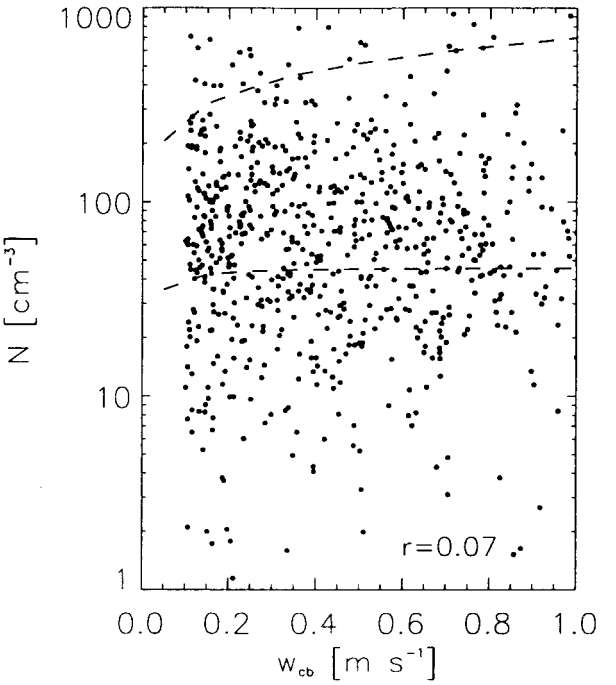

Figure 1. N as a function of cloud base Doppler velocity w_{cb} (positive values only) for all data. The correlation coefficient for these data is 0.07. Superimposed are theoretical calculations of N versus w_{cb} derived from an adiabatic parcel model representing droplet activation for two different CCN input spectra: (1) a narrow spectrum with a concentration of 1000 cm^{-3} and median radius of 0.05 μm (top curve), and (2) a broad spectrum with a concentration of 50 cm^{-3} and median radius of 0.1 μm (bottom curve).

Table 1. Summary of Six ASTEX Cases

Day in June	Duration, T	Drizzle
12	1200–2400	yes
13	1200–2200	no
14	0000–1200	no
17 (am)	0000–1200	yes
17 (pm)	1200–2400	yes
18	0000–1200	no

The duration of each case is indicated in UT; am, before noon; pm, after noon.

Further analysis has been performed to examine the relationship between N and cloud turbulence, as represented by σ_w^2. In calculating σ_w^2, $\bar{w}$ has first been calculated over 25 min intervals and then (2) has been applied. Figure 3a shows N versus the cloud-averaged σ_w^2 for all events. It is noted that there is a fairly significant positive correlation between N and σ_w^2 ($r = 0.56$). Analysis of only nondrizzling days shows a weaker but still significant positive correlation ($r = 0.45$) between these parameters (Figure 3b), while drizzling days (Figure 3c) exhibit a weaker positive correlation ($r = 0.38$). Note that the fact that the correlation between N and σ_w^2 is highest for the entire data set is in part due to the expanded range of data points included in the calculation.

Finally, to test how robust this feature is, an analysis was performed for the entire duration of each case (Figure 4). There is a tendency for N to increase with σ_w^2, although the days that experienced drizzle exhibit a fair amount of variability in N for similar σ_w^2. In general, however, the days during which the highest N were recorded (June 13 and June 14) are also the days during which the highest values of σ_w^2 were recorded. The tendency for N to increase with increasing σ_w^2 shown in Figures 3 and 4 is at least qualitatively similar to *Leaitch et al.* [1996].

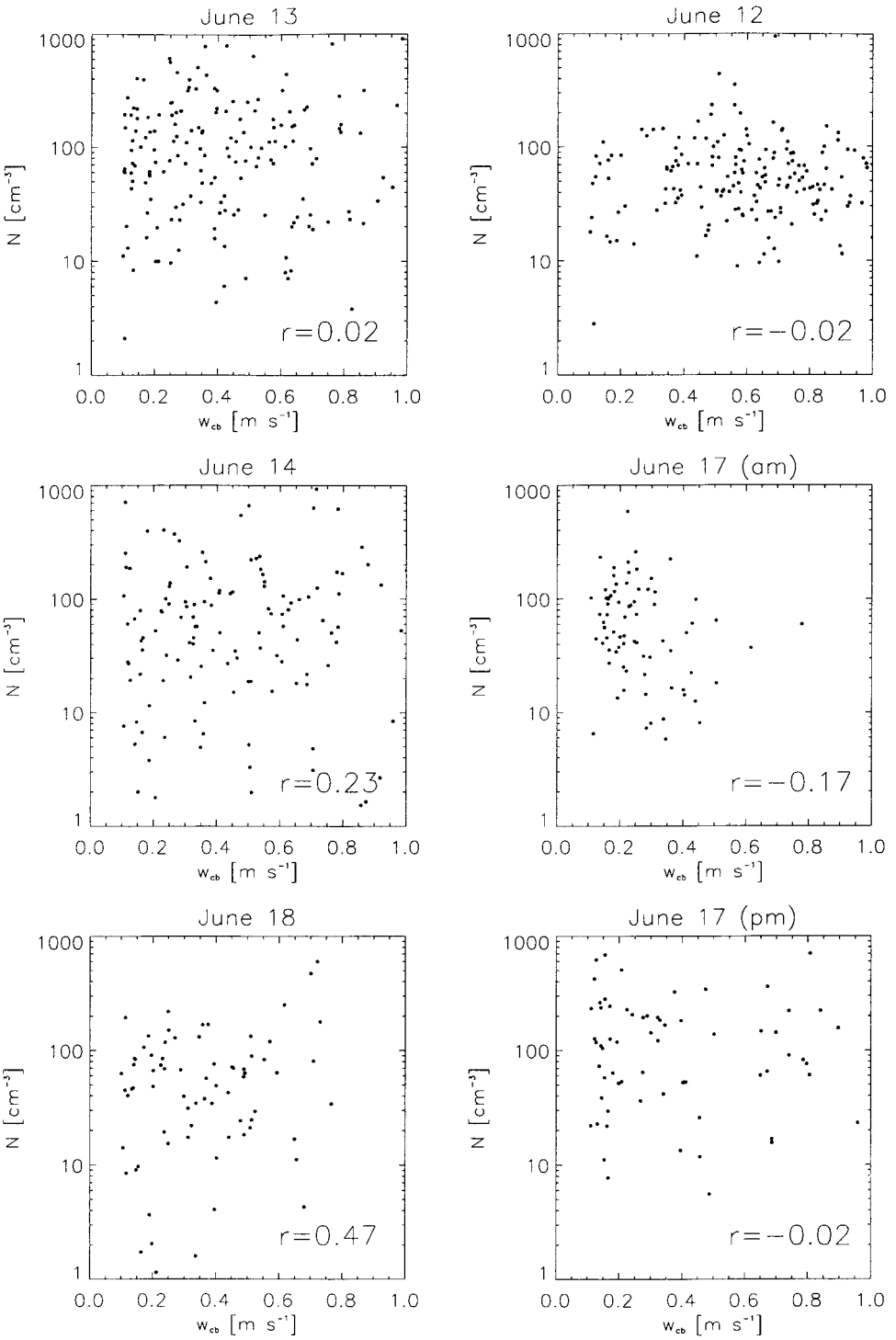

Figure 2. As in Figure 1 but for data separated by case. The figures in the left column are all nondrizzling days, whereas those in the right column are for drizzling days. Correlation coefficients are indicated in each plot.

3.2. Relationship Between σ_w^2 and Drizzle Formation

In focusing on this issue we first illustrate the differences between a nondrizzling and a drizzling day by comparing June 18 and June 17 (after noon). Figure 5 shows mean 12 hour profiles for each of these events and indicates that for the nondrizzling day (June 18), σ_w^2 is generally higher than for the drizzling day (June 17). Although June 18 exhibits a σ_w^2 profile with multiple maxima, the absolute maximum is in the cloudy region ($z/z_i > 0.8$, where z is height and z_i is cloud top) close to cloud top. The secondary maxima exist below cloud base and are of similar order of magnitude to the cloud top peak. On June 17 there is a distinct peak in σ_w^2 in the lower part of the boundary layer and a much smaller in-cloud peak. Perhaps more noteworthy is the fact that on June 18 the Z and σ_w^2 profiles are well correlated for $z/z_i > 0.6$, whereas there appears to be a negative correlation between the two fields on

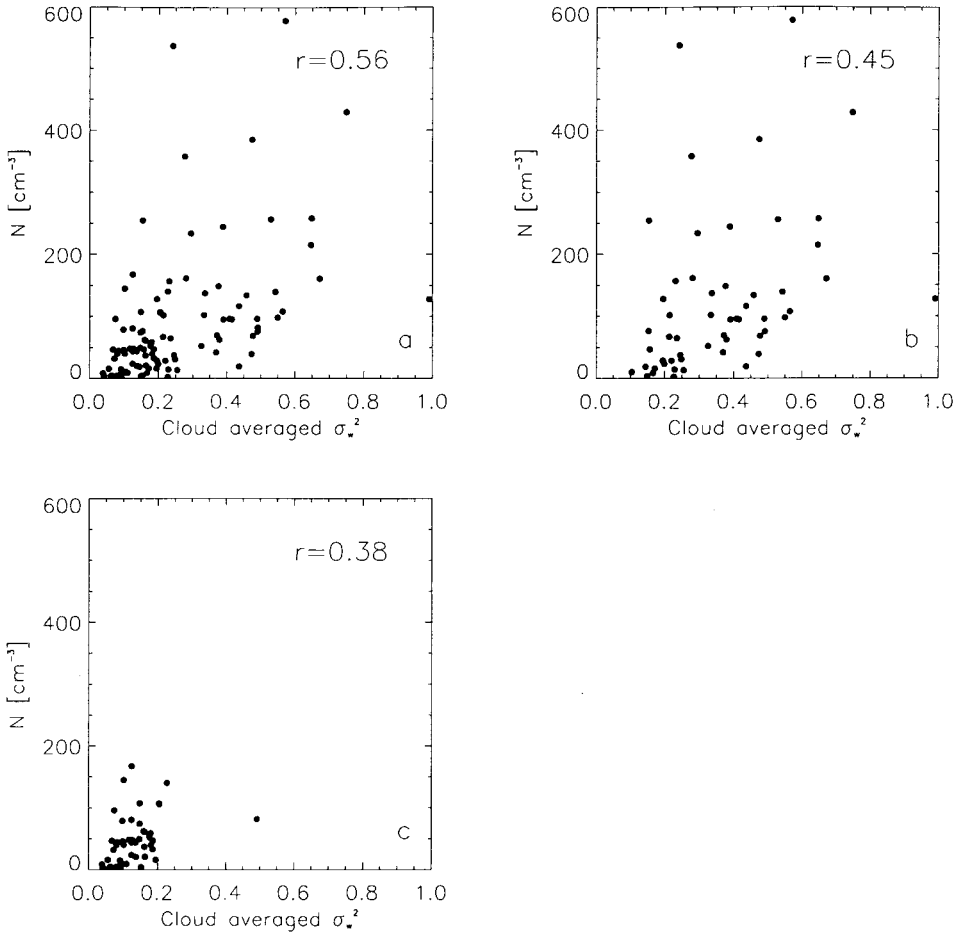

Figure 3. N as a function of mean cloud σ_w^2 for (a) all data, (b) nondrizzling days, and (c) drizzling days. Data have been averaged over 25 min periods. Correlation coefficients are indicated in each plot.

June 17 for $z/z_i < 0.8$ (Figure 5b). To put these data in perspective for all of the days studied, we show the correlation between σ_w^2 and Z (Figure 6) for (Figure 6a) the upper 20% and (Figure 6b) the lower 80% of the boundary layer. The choice of the 80/20% split captures roughly the split between cloud-free air and cloudy air. Analyses with a 70/30% split yielded qualitatively similar results. Note that there is a significant positive correlation between σ_w^2 and Z in the upper 20% of the boundary layer on all the nondrizzling days. Two of the drizzling cases (June 17 before noon and June 17 after noon) also show significant positive correlation between these parameters. In the lower 80% of the boundary layer, there is a negative correlation between σ_w^2 and Z on all the drizzling days, whereas the nondrizzling days show no clear trend. (See section 4.3 for further discussion.)

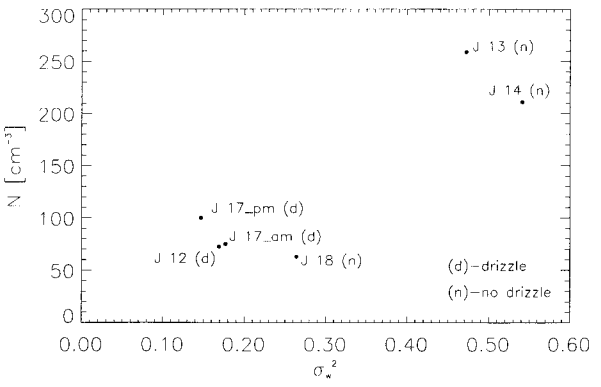

Figure 4. N as a function of mean cloud σ_w^2. Each data point represents the average value for a given case as labeled in the figure. The $(n)s$ indicate nondrizzling days, while the $(d)s$ indicate drizzling days.

To explore the relationship between σ_w^2 and Z further, we seek the cloud-averaged reflectivity Z (considered an indicator of the ability of a cloud to produce drizzle) from the time-averaged profiles (e.g., Figure 5) and plot it as a function of the cloud-averaged σ_w^2 (Figure 7). It can be seen that nondrizzling days tend to group into a region of low Z and high σ_w^2, whereas drizzling days group into the region of high Z and low σ_w^2.

4. Discussion

4.1. Correlation Between N and σ_w^2 and N and w_{cb}

Leaitch et al. [1996] presented analyses of N versus σ_w^2 based on aircraft data from stratus clouds sampled during the North Atlantic Regional Experiment. Their results indicated N increasing with σ_w^2 in a manner that is qualitatively similar to results in Figure 3. During ASTEX, *Feingold et al.* [1998] inferred CCN activation spectra from the same remote sensors employed in this study and found that for the case examined

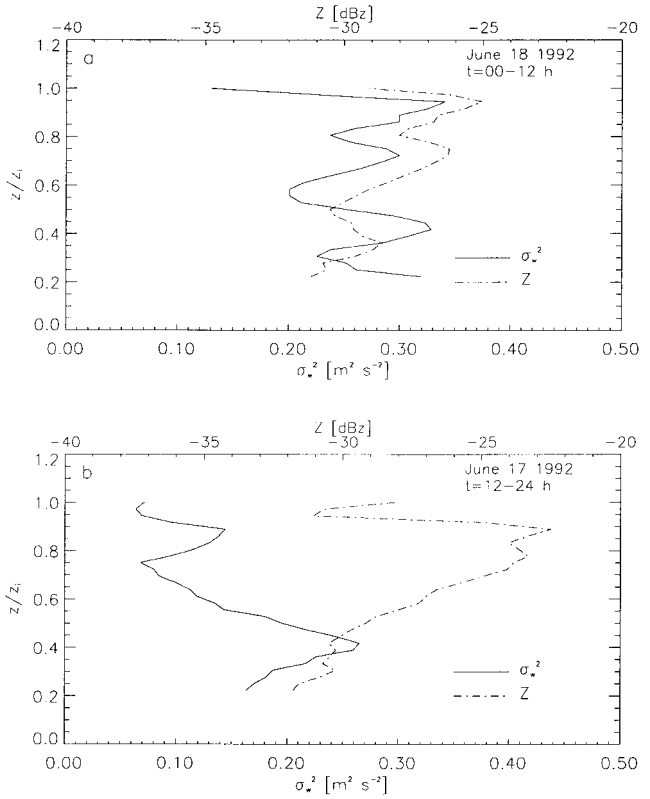

Figure 5. Profiles of σ_w^2 and Z averaged over 12 hours for (a) a nondrizzling boundary layer and (b) a boundary layer that has experienced drizzle.

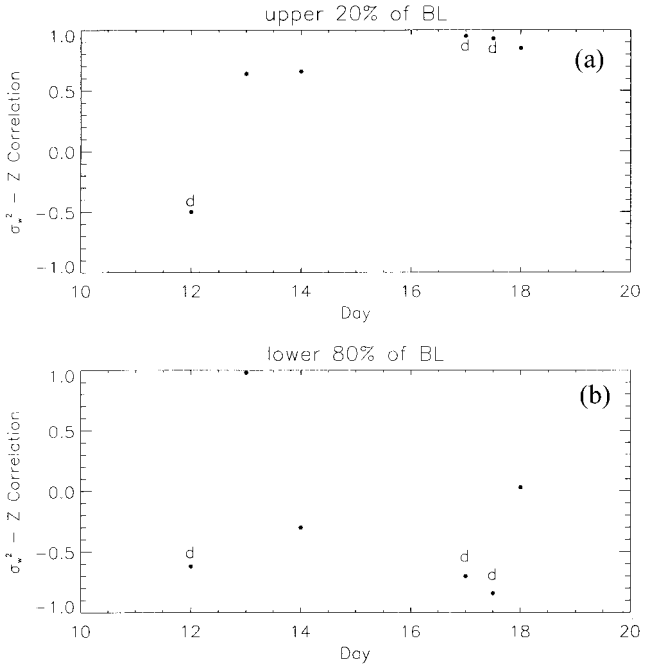

Figure 6. Correlation coefficients for (a) the upper 20% of the boundary layer and (b) the lower 80% of the boundary layer, as a function of the day of the experiment. Days that experienced drizzle are indicated with a "d." On most days there is a strong positive correlation between Z and σ_w^2 in the upper 20% of the boundary layer, whereas on days that have experienced drizzle, there is a strong negative correlation between these parameters in the lower 80% of the boundary layer.

(June 22, which is not one of the cases examined here), CCN spectra appeared to have rather steep slopes ($k \approx 1.5$). *Hudson and Frisbie* [1991] arrived at similar conclusions from their marine boundary layer measurements during the First ISCCP (International Satellite Cloud Climatology Project) Regional Experiment (FIRE-1). So although N has traditionally been regarded as more closely related to the number concentration of CCN (i.e., C) it appears that cloud dynamics may in some cases play a significant role in determining drop concentrations.

In the current analysis the fact that the retrieval of N is sensitive to the assumed breadth of the drop spectrum suggests that temporal averaging is in order. The values of N averaged over 25 min periods are well correlated with the in-cloud σ_w^2 calculated according to (2) for both nondrizzling and drizzling days. Even longer time averages still indicate that the highest values of N are associated with the highest values of in-cloud σ_w^2, so this result is robust.

The weak positive correlation or lack of correlation between N and w_{cb} raises a number of questions and does not necessarily indicate that w_{cb} is not a significant parameter determining droplet activation. The remote sensing technique may not have fine enough spatial resolution to resolve the scales on which droplet activation is occurring. As discussed in section 2.2, the retrievals of N are constrained by the 1 min temporal resolution of the microwave radiometer. This temporal resolution is equivalent to length scales of a few hundred meters and may not be sufficient to resolve the link between expansion and cooling in an updraft and the resultant activation of droplets. Nevertheless, the fact that there is a positive correlation between w_{cb} and N on at least two of the nondrizzling days exhibiting more of the classical features of a stratus deck suggests that the measurements may actually be capturing this process. To address the interaction of N and w_{cb}, one would ideally like to examine the relationship over a range of spatial scales to establish the most relevant scale. To do this, sampling at higher temporal resolution would have been necessary. The only way that this can be achieved with the current data set would be through interpolation of the LWP measurements to time intervals smaller than 1 min, but this would be ill-advised. It is suggested that future field experiments should acquire the relevant data at higher temporal/spatial resolution to explore this question further.

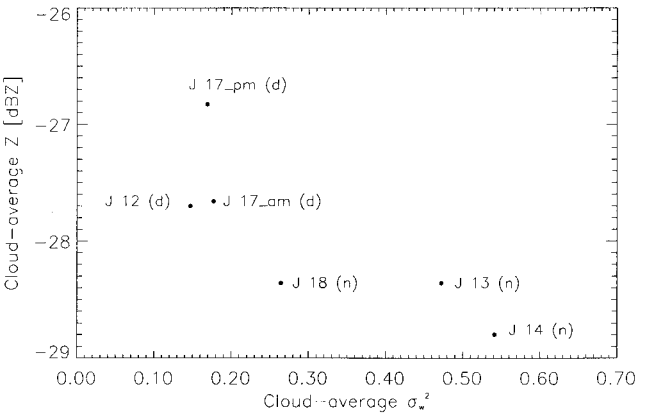

Figure 7. Cloud-averaged Z from the profiles in Figure 7 as a function of cloud-averaged σ_w^2. Nondrizzling days tend to have higher σ_w^2 and low Z, whereas days that have experienced drizzle tend to have higher Z and lower σ_w^2.

On drizzling days the lack of correlation between N and w_{cb} may indicate that droplet activation is occurring within convective updrafts that penetrate up into the stratus layer, or perhaps detrain to form the stratus layer. Since these updraft cores cover much smaller areas than the stratus deck itself, they are undersampled when temporal averaging is long, so the sampled cloud base tends to be at the base of the stratus deck rather than at the base of the cumulus clouds. Thus even if N and w are positively correlated within these cores, this is not detected by the analysis.

4.2. Correlation Between Z and σ_w^2 and Implications for Droplet Growth

Figure 6 indicates that there is, in general, a positive correlation between in-cloud turbulence (as represented by σ_w^2) and radar reflectivity Z. A number of possible explanations for this exist: Firstly, clouds that are more vigorous tend to have more liquid water because they penetrate higher, and for a given (constant-with-height) N, there is a greater chance of generating larger drops, and commensurately higher Z, with increasing distance above cloud base. The observations of *Martin et al*. [1995] show instances where penetrating turrets associated with cumulus penetrations of a stratocumulus deck have higher LWC but higher N and lower effective radius. Despite a lower effective radius, these situations could be characterized by higher Z than the surrounding cloud because of the higher LWC. There may be situations where a greater penetration height results in stronger entrainment and a reduction in LWC. The effect on Z is unclear; two factors need to be considered: (1) the depleted LWC at a greater penetration height may be larger than the undepleted LWC at a lower penetration height; and (2) the effective radius (or more precisely the tail of the drop spectrum) needs to be characterized to determine Z. The measurements in stratocumulus made by *Slingo et al*. [1982] suggest that cloud top effective radii are not affected by entrainment, which might be indicative of an inhomogeneous mixing process. In such cases, larger drops may still be present at cloud top, even if LWC is depleted by entrainment.

An alternative explanation is more dynamical in nature: clouds that have higher levels of turbulence kinetic energy (TKE) are expected to be able to support droplets within the cloud for longer periods of time [e.g., *Mason*, 1952]. These higher in-cloud residence times are likely associated with repeated circulations within the cloud, enabling the few larger droplets with radii greater than 20 μm to collect small droplets. This collision-coalescence mechanism is the dominant means by which precipitation-sized droplets are produced. *Feingold et al*. [1996] used a two-dimensional eddy-resolving model coupled to a model that explicitly resolved droplet growth to simulate an ASTEX stratocumulus case. They showed that longer in-cloud residence times are indeed responsible for prolonged drop growth and higher Z. Determining which of these explanations is most plausible would require sorting data having similar liquid water contents (or liquid water paths) but different levels of turbulence. Because of the temporal averaging required to calculate σ_w^2, the current data set would not yield sufficient data points to warrant such an exercise.

4.3. Impact of Drizzle on Boundary Layer Dynamics

As shown in Figure 7, boundary layers that have experienced drizzle tend to have higher cloud-average Z and lower cloud-average σ_w^2, while those that have not experienced drizzle have lower cloud-average Z and higher cloud-average σ_w^2. (See also Figure 5.) There is at least circumstantial evidence that this is linked to the distinct differences in the nature of boundary layers that have or have not experienced drizzle. *Paluch and Lenschow* [1991] and *Stevens et al*. [1998] showed that the evaporation of precipitation results in surface cooling and stabilization of the boundary layer. Boundary layers that have experienced precipitation tend, on average, to have rather weak motions that do not circulate through the depth of the boundary layer, with the exception of narrow, spatially intermittent, updraft cores associated with penetrating cumulus. Boundary layers that do not experience drizzle tend to have stronger motions that circulate through a greater depth of the boundary layer. Profiles of potential temperature θ for June 18 and June 17 after noon (Figure 8) corroborate this by showing that the boundary layer on the drizzling day (June 17 after noon) is more stable than that on the nondrizzling day (June 18). Therefore it appears from Figure 7 that the high Z and low σ_w^2 on drizzling days emanates from the cloud's enhanced ability to generate drizzle, together with the weaker circulations resulting from drizzle. On nondrizzling days the cases have lower Z (diminished ability to produce drizzle) and higher σ_w^2, indicative of stronger circulations.

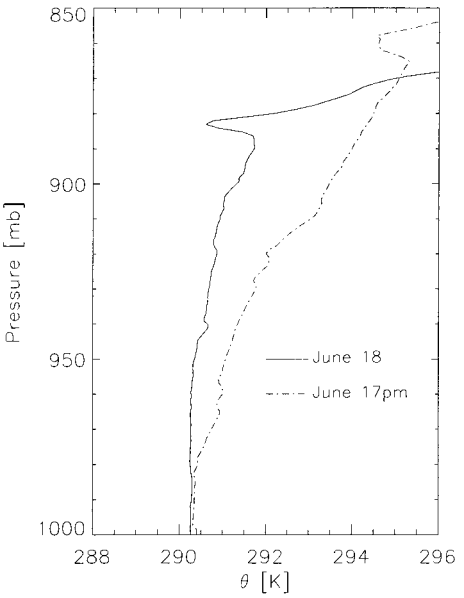

Figure 8. Representative profiles of potential temperature θ for a nondrizzling day (June 18) and a drizzling day (June 17 after noon). Profiles are derived from individual radiosondes launched some time in the middle of the event. Note the more stable profile on the drizzling day.

The existence of local penetrating cumuli generated in the aftermath of drizzle events, and the nature of their sampling by the radar, may also explain the negative correlation between Z and σ_w^2 observed in the subcloud region on drizzling days (Figure 6). This region is generally undersampled because of the absence of scatterers, so the average signal below cloud may be biased toward the spatially intermittent penetrating cumuli. Because these cumuli consist of newly activated, small droplets, Z is low in this region, and because they typically have fairly strong updrafts (order of 1 m s^{-1}), the resultant correlation is negative. Figure 5b illustrates this point rather well; the boundary layer shows a maximum in σ_w^2 below cloud at $z/z_i = 0.4$ in a region where Z is only about -30 dBZ.

Finally, it should be mentioned that we have not considered the possible role of shortwave radiation in this analysis. This was explored by *Frisch et al*. [1995a] who analyzed the data from June 17 and compared daytime and nighttime σ_w^2 profiles. Both profiles exhibited two maxima, one near cloud top and the other below cloud base. The nighttime σ_w^2 profile had a stronger cloud-top maximum than the daytime profile, probably because during the day, shortwave reduces turbulence generation by diminishing cloud-top longwave cooling. The daytime σ_w^2 profile showed a stronger maximum below cloud due to convective heating from below. Clearly, shortwave radiation does affect the σ_w^2 profiles, but because all cases in this study include both daytime and nighttime periods, the role of shortwave radiation cannot be separated from that of drizzle.

5. Summary and Conclusions

The combination of radar, microwave radiometer, and ceilometer/lidar provide an effective means for simultaneously measuring both cloud microphysical, and dynamical parameters. Data acquired by these instruments during ASTEX have been used here to address the relationships between cloud dynamics and droplet activation, and cloud/boundary layer dynamics and drizzle. Data have been separated into nondrizzling and drizzling days to investigate whether the boundary layers differ in any systematic way.

During the course of this analysis, it has become clear that it would have been desirable to have had higher temporal resolution in the microwave radiometer measurements so that the microphysical retrieval of N could have been performed at the resolution of the Doppler velocity measurements. This would then have enabled an analysis of the spatial scales at which it is desirable to represent the relationship between N and w. In addition, high (temporal) resolution spectral moments of the Doppler velocity spectrum would have alleviated the need to perform long time averaging of the data to calculate σ_w^2. This being said, we feel that the analysis performed here on the temporally averaged data is meaningful because certain features have emerged despite the averaging. The main results are summarized below.

1. For the combined data set there is no correlation between the drop number concentration and the cloud-base updraft velocity. However, on two of the three nonprecipitating days (June 14 and June 18) exhibiting more of the classical features of a stratus deck the correlation between cloud-base velocity and N was positive ($r = 0.47$ and $r = 0.23$). Drizzling days always exhibited either no correlation or negative correlation between N and cloud-base updraft velocity.

2. On both drizzling days and nondrizzling days there is a significant positive correlation ($r = 0.38 - 0.56$) between N and σ_w^2, confirming a prior study based on in situ aircraft measurements [*Leaitch et al*., 1996].

3. There is a strong correlation between radar reflectivity Z and in-cloud turbulence σ_w^2 on all the nondrizzling days and on some of the drizzling days. The source of this correlation could be related to the fact that more turbulent clouds are more strongly forced, penetrate higher, and contain more liquid water. Alternatively, it could indicate that clouds with higher turbulence can support droplets in cloud for longer and allow for enhanced droplet growth.

4. On drizzling days, boundary layers are characterized by higher in-cloud Z and lower in-cloud σ_w^2; conversely, on nondrizzling days, boundary layers are characterized by lower in-cloud Z and higher in-cloud σ_w^2. This is consistent with prior studies [*Paluch and Lenschow*, 1991; *Stevens et al*., 1998] which show that the evaporation of drizzle tends to stabilize the boundary layer by cooling the surface layer, thus suppressing boundary layer motions.

5. In the subcloud region, Z and σ_w^2 are negatively correlated on drizzling days. In the aftermath of drizzle, convective cores tend to penetrate the boundary layer and stratus deck, and in the subcloud region, they dominate the radar signal. These cores have fairly high σ_w^2 but rather low Z because the newly formed drops are small.

We are of the opinion that although quantitative retrievals using remote sensors are difficult, these large data sets will become increasingly valuable as a means of addressing cloud dynamical/microphysical problems, especially if temporal/spatial resolution is improved. Data of this kind will be useful to climate modelers who often rely on poorly resolved vertical velocity fields to represent cloud formation.

Acknowledgments. The NOAA Environmental Technology Laboratory (ETL) radar and lidar groups are thanked for their efforts expended in acquiring this data set. In particular, thanks are due to J. Snider (ETL) who provided the microwave radiometer data. Comments by anonymous reviewers were helpful. Part of this work was funded by DOE/ARM under IAG-DE-A103-97ER62342 and 164514-A-91 and by the NOAA Office of Global Programs. WRC and GF received support from NSF grant ATM-9529321 entitled "Simulations of cloud/radiative responses to variations in CCN."

References

Atlas, D., The estimation of cloud parameters by radar, *J. Meteorol*., *11*, 309–317, 1954.

Austin, P. H., Y. Wang, R. Pincus, and V. Kujala, Precipitation in stratocumulus clouds: Observational and modelling results, *J. Atmos. Sci*., *52*, 2329–2352, 1995.

Bowen, E. G., The formation of rain by coalescence, *Aust. J. Sci. Res. A*, *3*, 193–213, 1950.

Feingold, G., B. Stevens, W. R. Cotton, and A. S. Frisch, On the relationship between drop in-cloud residence time and drizzle production in stratocumulus clouds, *J. Atmos. Sci*., *53*, 1108–1122, 1996.

Feingold, G., S. Yang, R. M. Hardesty, and W. R. Cotton, Retrieving cloud condensation nucleus properties from Doppler cloud radar, microwave radiometer, and lidar, *J. Atmos. Oceanic Technol*., *15*, 1189–1196, 1998.

Frisch, A. S., D. H. Lenschow, C. W. Fairall, W. H. Schubert, and J. S. Gibson, Doppler radar measurements of turbulence in marine stratiform cloud during ASTEX, *J. Atmos. Sci*., *52*, 2800–2808, 1995a.

Frisch, A. S., C. W. Fairall, and J. B. Snider, Measurement of stratus cloud and drizzle parameters with a K_α-band Doppler radar and a microwave radiometer, *J. Atmos. Sci*., *52*, 2788–2799, 1995b.

Frisch, A. S., B. Martner, I. Djalalova, and M. Poellet, Radar/radiometer retrievals of stratus cloud liquid water content profiles compared with in-situ measurements by aircraft, in *Proceedings of the Conference on Radar Meteorology*, *Am. Meteorol. Soc*., Boston, Mass., 1999.

Gibson, J. S., Simulated and measured spectral width estimates from a meteorological radar, M. S. thesis, Dep. of Appl. Math., Univ. of Colo., Boulder, 1988.

Hogg, D. C., M. T. Decker, F. O. Guiraud, K. B. Earnshaw, D. A. Merritt, K. P. Moran, W. B. Sweezy, R. G. Strauch, E. R. Westwater, and C. G. Little, A steerable dual-channel microwave radiometer for measurement of water vapor and liquid in the troposphere, *J. Clim. Appl. Meteorol*., *22*, 789–806, 1983.

Hudson, J. G., Cloud condensation nuclei measurements within clouds, *J. Clim. Appl. Meteorol*., *23*, 42–51, 1984.

Hudson, J. G., and P. R. Frisbie, Cloud condensation nuclei near marine stratus, *J. Geophys. Res*., *96*, 20,795–20,808, 1991.

Kropfli, R. A., S. Y. Matrosov, T. Uttal, B. W. Orr, A. S. Frisch, K. A. Clark, B. W. Bartram, R. F. Reinking, J. B. Snider, and B. E.

Martner, Cloud physics studies with 8 mm wavelength radar, *Atmos. Res*., *35*, 299–313, 1995.

Leaitch, W. R., C. M. Banic, G. A. Isaac, M. D. Couture, P. S. K. Liu, I. Gultepe, and S.-M. Li, Physical and chemical observations in marine stratus during the 1993 North Atlantic Regional Experiment: Factors controlling cloud droplet number concentrations, *J. Geophys. Res*., *101*, 29,123–29,135, 1996.

Lenschow, D. H., J. Mann, and L. Kristensen, How long is long enough when measuring fluxes and other turbulence statistics, *J. Atmos. Oceanic Technol*., *11*, 661–673, 1994.

Martin, G. M., D. W. Johnson, D. P. Rogers, P. R. Jonas, P. Minnis, and D. A. Hegg, Observations of the interaction between cumulus clouds and warm stratocumulus clouds in the marine boundary layer during ASTEX, *J. Atmos. Sci*., *52*, 2902–2922, 1995.

Mason, B. J., Production of rain and drizzle by coalescence in stratiform clouds, *Q. J. R. Meteorol. Soc*., *78*, 377–386, 1952.

Nicholls, S., The dynamics of stratocumulus, *Q. J. R. Meteorol. Soc*., *110*, 821–845, 1984.

Paluch, I. R., and D. H. Lenschow, Stratiform cloud formation in the marine boundary layer, *J. Atmos. Sci*., *48*, 2141–2157, 1991.

Paluch, I. R., C. A. Knight, and L. J. Miller, Cloud liquid water and radar reflectivity of nonprecipitating cumulus clouds, *J. Atmos. Sci*., *53*, 1587–1603, 1996.

Pearson, G. N., A high-pulse-repetition-frequency CO_2 Doppler lidar for atmospheric monitoring, *Rev. of Sci. Instrum*., *64*(5), 1155–1157, 1993.

Slingo, A., S. Nicholls, and J. Schmetz, Aircraft observations of marine stratocumulus during JASIN, *Q. J. R. Meteorol. Soc*., *108*, 833–856, 1982.

Stevens, B., W. R. Cotton, G. Feingold, and C.-H. Moeng, Large-eddy simulations of strongly precipitating, shallow, stratocumulus-topped boundary layers, *J. Atmos. Sci*., *55*, 3616–3638, 1998.

Twomey, S., The nuclei of natural cloud formation, II, The supersaturation in natural clouds and the variation of cloud droplet concentration, *Geofis. Pura Appl*., *43*, 243–249, 1959.

Twomey, S., *The Atmospheric Aerosol*., 302 pp., Elsevier, New York, 1977.

W. R. Cotton, Department of Atmospheric Science, Colorado State University, Fort Collins, CO 80523.

G. Feingold and A. S. Frisch, Cooperative Institute for Research in the Atmosphere/NOAA, Environmental Technology Laboratory, 325 Broadway, Boulder, CO 80303. (gfeingold@etl.noaa.gov)

B. Stevens, Department of Atmospheric Sciences, University of California, Los Angeles, CA 90095.

(Received December 4, 1998; revised June 18, 1999;
accepted June 23, 1999.)